Assessment of Wearable Lower Limb Rehabilitation Robot Dynamics: A Study on ROM Training Performance

J. Annisa ; S. Mohamaddan ; M.A. Zulkifli ; H. Hazmi ; M.N. Lemon All Authors

Abstract:

A wearable lower limb rehabilitation robot (WLLR) is one of the effective ways to assist a stroke patient who has abnormal gait. The accuracy of the dynamic model is important as it relates to the performances of the robot to track the trajectory. Error in modelling can be magnified futher resulting to poor tracking performance. However, the development of the dynamic model for WLLR is challenging because the structure is highly non-linear and heavily coupled. In this paper, a mathematical modelling for an improved design of wearable lower limb rehabilitation robot (WLLR) is presented. The Lagrangian formulation was utilized to derive the dynamic model of the hip and knee joint. Simple PID (Ziegler–Nichols) based controller was developed in order to verify the developed dynamic model. MATLAB SimMechanic software was used to simulate the WLLR motion behaviour to imitate a real environment. The results demonstrate the successful tracking of desired ranges of motion (ROM) by WLLR joints with low rise time and steady-state error. Thus, the developed dynamic model is acceptable and can be utilized for future improvement of the controller systems for WLRR.

Published in: 2023 IEEE 9th International Conference on Smart Instrumentation, Measurement and Applications (ICSIMA)

Date of Conference: 17-19 October 2023

DOI: 10.1109/ICSIMA59853.2023.10373433

Date Added to IEEE Xplore: 03 January 2024

Publisher: IEEE

ISBN Information:

Conference Location: Kuala Lumpur, Malaysia

Assessment of Wearable Lower Limb Rehabilitation Robot Dynamics: A Study on ROM Training Performance

*J.Annisa
Department of Mechanical and Manufacturing Engineering, Faculty of Engineering
Universiti Malaysia Sarawak
Kota Samarahan, Sarawak, Malaysia
* email address: jannisa@unimas.my

M.A. Zulkifli
Department of Mechanical and Manufacturing Engineering, Faculty of Engineering
Universiti Malaysia Sarawak
Kota Samarahan, Sarawak, Malaysia
axiphzull@yahoo.com

M. N. Leman
Department of Mechanical and Manufacturing Engineering, Faculty of Engineering
Universiti Malaysia Sarawak
Kota Samarahan, Sarawak, Malaysia

S. Mohamaddan
Department of Bioscience and Engineering, College of System Engineering and Science
Shibaura Institute of Technology
Tokyo, Japan

H. Hazmi
Department of Community Medicine and Public Health
Faculty of Medicine and Health Sciences, Universiti Malaysia Sarawak
Kota Samarahan, Sarawak, Malaysia

2023 IEEE 9th International Conference on Smart Instrumentation, Measurement and Applications (ICSIMA) | 979-8-3503-4338-0/23/$31.00 ©2023 IEEE | DOI: 10.1109/ICSIMA59853.2023.10373433

***Abstract*— A wearable lower limb rehabilitation robot (WLLR) is one of the effective ways to assist a stroke patient who has abnormal gait. The accuracy of the dynamic model is important as it relates to the performances of the robot to track the trajectory. Error in modelling can be magnified futher resulting to poor tracking performance. However, the development of the dynamic model for WLLR is challenging because the structure is highly non-linear and heavily coupled. In this paper, a mathematical modelling for an improved design of wearable lower limb rehabilitation robot (WLLR) is presented. The Lagrangian formulation was utilized to derive the dynamic model of the hip and knee joint. Simple PID (Ziegler–Nichols) based controller was developed in order to verify the developed dynamic model. MATLAB SimMechanic software was used to simulate the WLLR motion behaviour to imitate a real environment. The results demonstrate the successful tracking of desired ranges of motion (ROM) by WLLR joints with low rise time and steady-state error. Thus, the developed dynamic model is acceptable and can be utilized for future improvement of the controller systems for WLRR.**

Keywords—Wearable Robot, SimMecahnics, Lower Limb, Rehabilitation Robot, ROM Training.

I. INTRODUCTION

Nowadays, many types of lower limb rehabilitation robot (LLRRs) have been invented by researches worldwide. The rehabilitation robot has two types of groups: the exoskeleton and end-effector robot [1,2]. Treadmill and wearable-based robots are exampls of the exoskeleton [3] while the footplate- and platform-based robots belongs to the end-effector group.

The treadmill-based robot, an exoskeleton robot has a bodyweight support system. During the rehabilitation on the treadmill, patients' wear the body weight support system by fitting the exoskeleton robot to their lower limb. The body weight support system functions to support the patient, preventing them from fall during treatment. The benefit of treadmill based robot is, it reduces the energy expenditure. However, the treadmill based robots often require therapists to assist the patients during treatment. Additional problems to the readmill based robots include the patients' limited movement. The contraption that patients wear prevents free movement and maybe uncomfortable to the wearer during rehabilitation.

A wearable lower limb rehabilitation robot (WLLR) is a mechanical system that is worn to provide assistance to the patients while walking. The current design is bulky, with non-user friendly control scheme, making it inappropriate for home use or application. Most existing LLRR were designed with fix kinematic structure and to carry out very specific task, for example, performing passive or active gait treatment only but excluding the passive or active limb joint training [4]. These factors limit its adaptability to different users' need and tasks.

Among all available LLLR, the wearable-based robot is preferable because it is designed to fit the patients' lower limb and provide power assistance while walking. Hence, patients can walk freely while receiving treatment. Many wearable robots have been developed by researchers worldwide in order to help patients to perform rehabilitation treatment [5-7]. Bortole et al. [8] developed the robotic exoskeleton, namely H2 for stroke patients. The robot has 6 DOFs which allow intensive overground gait training. Early findings demonstrated that H2 appears to be safe, easy to use and can be used to conduct intensive gait training for hemiparestic stroke survivor. Chen et al. [9] developed a 7 DOFs wearable robot, called the CHUK-EXO for the patients with lower extremity paralysis. The CHUK-EXO has the ability to perform sit-to-stand (STS) and gait motions. Bartenbach et al. [10] developed a wearable robot with a system that uses 20 different sensors to measure alteration in gait kinematics, human-robot interaction forces and physical load. Thus, the robot has the advantage to be more flexible that improves the human robot interaction. Gan et al. [11] developed a wearable robot that focuses on giving the patient greater freedom of movement, convenience, and balance. Kim & Bae, [12] designed an exoskeleton robot that responds to the wearer's intentions and provide the required assistance instead of restraining the patient's motions. Direct force mode control was applied in the control strategy to allow higher level of human interaction to the robot. Hayner, [13] developed 6 DOFs wearable robot, called Ekso GT. The robot assists

patients with various levels of lower extremity weakness ranging from patients with a lower level of mobility disorder as in stroke survivors to the paralysed. Chen et al. [14] developed a flexible design wearable robot to assist patients who suffers from the abnormal gait. The design was based on a study of the movements of the lower limbs where the position and orientation of each joint during gait action was determined. The hybrid assistive limb (HAL) exoskeleton is both assistive and augmentative device manufactured by Cyberdyne Inc. The robot is controlled by two systems, namely "Cybernic Voluntary Control System" and "Cybernic Autonomous Control System" [15].

Despite all the progresses made, most of existing WLLR were designed only for a specific task and have fix kinematic structure which concentrates on either passive or active range of motion (ROM) training. The combination of both treatments is essential to ensure that the WLLR is more multipurpose, cost-saving and practical solution for home application. An improved design of wearable lower-limb robot (WLLR) for home-based application can be offered to cater for the aformentioned shortcomings. The accuracy of the improved dynamic model is vital for an effective control system of the WLLR. Inappropriate modelling can lead to large error resulting in reduced control tracking performance. Several methods have been proposed to represent the dynamic model of WLLR. They include artificial intelligent [16], human-machine coupled motion model [17], virtual multi-body model [18] and system identification method [19-20]. However, these methods require advanced level of knowledge in computation software, hardware setup and accurate experimental data. Mathematical modeling approach is the most widely used for dynamic modeling because it can be mathematically developed despite involving heavy mathematical derivation. The developed mathematical modeling can provide a prior knowledge on how the system work. In fact, the dynamic modeling derived mathematically can be used to develop a newer control system.

Thus, in this paper, a mathematical model for an improved design of wearable lower limb rehabilitation robot (WLLR) is presented. The Lagrangian formulation was utilized to derive the dynamic model of the hip and knee joint. Simple PID based controller was developed in order to verify the developed dynamic model. MATLAB Simmechanic software was used to simulate the WLLR motion behaviour in a real environment. This paper is organized as follows. The second section present the proposed design of WLLR. In the third section focuses on the dynamic modeling. And the last section emphasises on the PID controller and simulation.

II. WLLR Design

The modular configuration is adapted into the WLRR design as shown in Fig.1. This concept allows the WLLR to perform several basic movements for the lower limb treatment. The movements include ROM exercise and walking gait treatment. It can be achieved by only changing the robot configuration or the usage of external accessories. The proposed WLLR can be configured by five main configurations, and the possible configurations is shown in Fig. 2. C1 and C2 are configured for walking gait training with or without passive ankle, respectively. The training includes a flexion/extension of hip and knee joint in passive and active mode. Meanwhile, C3 and C4 are concentrated on ROM training of hip and knee for right and left leg, respectively. This training is essential to improve the patients' range of motion (ROM) before undergoing active training while C5 is concentrated on passive ankle training focusing on dorsiflexion/plantarflexion.

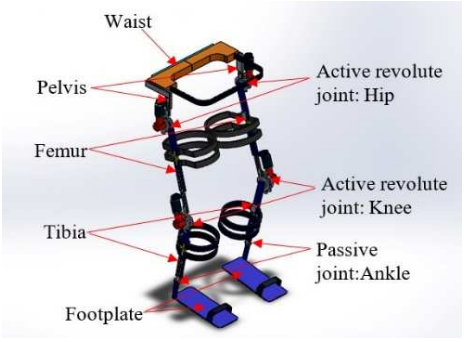

Fig. 1. WLLR Design

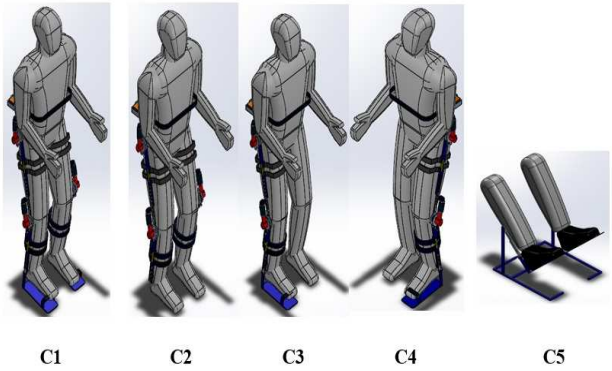

Fig. 2. WLLR Configurations

III. Dynamic Model

A. Dynamic Model of WLRR Structure

The WLLR design has two active hip joint, two active knee joint and two passive ankles joint with the total six DOFs. Similar to kinematic analysis, only active revolute joints are taken into consideration. Since both legs have the same kinematic structure, only a single leg is analysed.

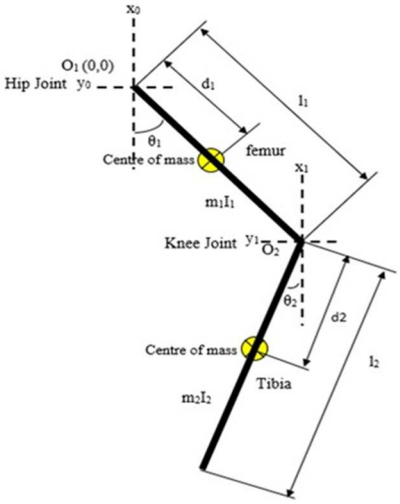

Fig. 3. Free Body Diagram of the WLLR Structure

Based on these assumptions, the free-body diagram of the WLLR structure in the sagittal plane arrangment is simplified

as in Fig. 3 which is O_1 and O_2 represent hip and knee origin axis. l_1 and l_2 represent the length of femur and tibia, d_1 and d_2, respectively represent the distance between O1 and O2 to the centre of gravity (CG) of femur and tibia. Meanwhile, m_1 and m_2 represent the mass of femur and tibia while $I_1$and I_2 is the inertia of femur and tibia structure respectively. The torque for each joint is modelled by using Lagrangian formulation as in (1) and (2).

While E_p and E_k are the total potential and kinetic energy respectively. The relation of $E_p$and $E_k$in Lagrangian function is written as follows;

$$L_a = E_p - E_k \tag{1}$$

$$T_{li} = \frac{d}{dt}\left(\frac{\partial L_a}{\partial \dot{\theta}_i}\right) - \left(\frac{\partial L_a}{\partial \theta_i}\right) \tag{2}$$

$$E_p = \sum_{i=1}^{2} m_i\, g y_i \tag{3}$$

$$E_k = \sum_{i=1}^{2} \left[\frac{1}{2} m_i (\dot{x}_i^2 + \dot{y}_i^2) + \frac{1}{2} I_i \dot{\theta}_i^2\right] \tag{4}$$

Where m_i and I_i are the mass and inertia of each femur and tibia, g is the gravity acceleration. The location of (CG) is representing by (x_i, y_i)which is derived by geometric relation presented as in the following equation;

$$x_i = \sum_{j=1}^{i-1} l_j \sin(\theta_i) + d_i \sin(\theta_i) \tag{5}$$

$$y_i = \sum_{j=1}^{i-1} -l_j \cos(\theta_i) - d_i \cos(\theta_i) \tag{6}$$

l_j is a length of femur or tibia and d_i is the distance of the femur or tibia to (CG). The derivative of the equation above is expressed as in (7) and (8).

$$\dot{x}_i = \sum_{j=1}^{i-1} I_j\, \dot{\theta}_j(\cos\theta_j) + d_i\, \dot{\theta}_i(\cos\theta_i) \tag{7}$$

$$\dot{y}_i = \sum_{j=1}^{i-1} I_j\, \dot{\theta}_j(\sin\theta_j) + d_i\, \dot{\theta}_i(\sin\theta_i) \tag{8}$$

Where $\dot{x}_i$and $\dot{y}_i$ are the angular velocity of CG. By using (1) until (8), the torque equation for the hip and knee joint are obtained as follows;

$$T_{l1} = m_1 d_1^2 \ddot{\theta}_1 + I_1 \ddot{\theta}_1 + m_2 l_1^2 \ddot{\theta}_1 + m_2 l_1 d_2 \ddot{\theta}_2 \cos(\theta_2 - \theta_1) + m_2 l_1 d_2 \dot{\theta}_2^2 \sin(\theta_2 - \theta_1) + m_1 g d_1 \sin(\theta_1) + m_2 g l_1 \sin(\theta_1) \tag{9}$$

$$T_{l2} = m_2 d_2^2 \ddot{\theta}_2 + I_2 \ddot{\theta}_2 + m_2 l_1^2 \ddot{\theta}_1 + m_2 l_1 d_2 \ddot{\theta}_1 \cos(\theta_2 - \theta_1) + m_2 l_1 d_2 \dot{\theta}_1^2 \sin(\theta_2 - \theta_1) + m_2 g d_2 \sin(\theta_2) \tag{10}$$

In order to linearize and simplifying torque of hip (T_{l1}) and knee (T_{l2}), the performance of the WLLR joint is established under ROM condition in which one joint keeps moving while the other joint is fixed [21,22]. It means that when the knee joint moves, the position changes (θ_2)then, angular velocity $(\dot{\theta}_2)$ and angular acceleration $(\ddot{\theta}_2)$ of the knee joint are equal to zero. Similarly, when the hip joint moves, the position changes (θ_1), then, angular velocity $(\dot{\theta}_1)$, and angular acceleration$(\ddot{\theta}_1)$ of the hip joint are equal to zero. By applying the condition torque for hip(T_1) and knee(T_2) under the range of motion(ROM), (9) and (10) can be simplified as follows;

$$T_{l1} = (m_1 d_1^2 + I_1 + m_2 l_1^2)\ddot{\theta}_1 + (m_1 g d_1 + m_2 g l_1)\, sin(\theta_1) \tag{11}$$

$$T_{l1} = (m_1 d_1^2 + I_1 + m_2 l_1^2)\ddot{\theta}_1 + (m_1 g d_1 + m_2 g l_1)\, sin(\theta_1) \tag{12}$$

B. Dynamic Model of WLRR System

Direct current (DC) brushed motor is selected as an actuator for the WLLR hip and knee joint. It is because the DC motor meets the criteria of necessary power with a compact and portable solution for a wearable robot. A gearbox is coupled with a rotary shaft to reduce the angular velocity and increase torque generated by the DC motor. The output of the gearbox produce rotation to the shaft, that is fixed to the WLLR link. The motor components consist of resistance and inductance, which allow converting the electrical to mechanical energy to provide torque for joint rotation. The mathematical model of the DC motor by applying Kirchhoff's law is written as follows;

$$U_i - V_{emfi} = R_{mi} i_i + L_{mi}\left(\frac{di}{dt}\right) \quad i = 1,\ 2 \tag{13}$$

Where, L_{mi} is the motor inductance, R_{mi} is resistance and $i$is current of the motor. U_i is the circuit input voltage, and V_{emfi} is the back electromotive force voltage which is the value is proportional to the motor shaft angular velocity. The relation is shown in (14).

$$V_{emfi} = K_{bi} \dot{\theta}_{shfi} \quad i = 1,\ 2 \tag{14}$$

K_{bi} is the motor voltage constant and $\dot{\theta}_{shfi}$ is the angular velocity of the gear shaft. The output of the motor is a torque which rotates the shaft proportional to the current, $i$as in (15)

$$T_{mi} = K_{mi} i_i \quad i = 1,\ 2 \tag{15}$$

Where, K_{mi} is motor torque sensitivity while T_{mi} is the torque applied to the motor. By substituting (14) and (15) into (28), the mathematical model of the motor in Laplace is represented in (16).

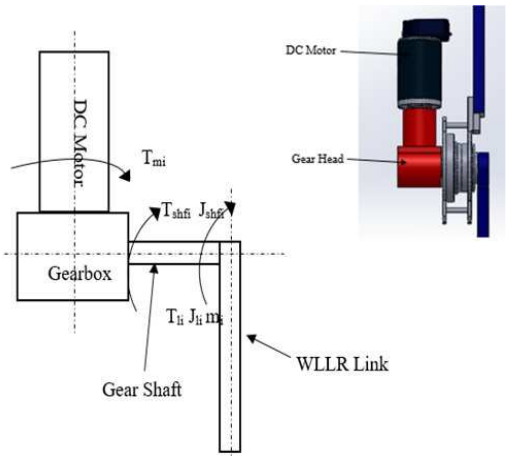

Fig. 4. WLLR Hip and Knee Joint

$$U_i(s) - K_{bi}s\theta_{shfi}(s) = \frac{(L_{mi}s+R_{mi})T_{mi}(s)}{K_{mi}} \quad (16)$$

T_{mi} can be obtained based on the ratio of the gear correlates with the input and output torque is given in (32).

$$r_g = \frac{T_{out}}{T_{in}} = \frac{N_{out}}{N_{in}} \quad (17)$$

Where r_g is the gearbox ratio, T_{out} and T_{in} are the output and input torque of the gearbox and motor. Thus, N_{out} and N_{in} are the numbers of teeth for output and input gears. The output and input torque of the joint base in Fig. 4 is derived as in the following equation;

$$T_{ini} = T_{mi} \quad (18)$$

$$T_{outi} = T_{shfi} + T_{li} \quad (19)$$

T_{shfi} is the torque of the gearbox shaft while T_{mi} is torque generated by the DC motor. T_{li} represents the torque of femur and tibia link where (i=1,2) which is 1 for the hip and 2 for the knee. By substituting (18) and (19) into (17), the torque of the gearbox is written as (20) and the Laplace is written in (21).

$$T_{mi} = \frac{1}{r_g}\left(T_{shfi} + T_{li}\right) \quad (20)$$

$$T_{mi}(s) = \frac{1}{r_g}\left(T_{shfi}(s) + T_{li}(s)\right) \quad (21)$$

Where T_{li} is Laplace of (11) and (12) which is the torque for the hip and knee respectively is written as follow;

$$T_{l1}(s) = (m_1d_1^2 + I_1 + m_2l_1^2)s^2\theta_{shf1}(s) + (m_1gd_1 + m_2gl_1)\theta_{shf1}(s) \quad (22)$$

$$T_{l2}(s) = (m_2d_2^2 + I_2)s^2\theta_{shf2}(s) + (m_2gd_2)\theta_{shf2}(s) \quad (23)$$

The dynamic equations of the gear shaft for hip and knee joint T_{shfi} are expressed as in (24) and (25), and the Laplace is shown in (26) and (27) respectively.

$$T_{shf1} = J_{shf1}\ddot{\theta}_{shf1} + B_{shf1}\dot{\theta}_{shf1} \quad (24)$$

$$T_{shf2} = J_{shf2}\ddot{\theta}_{shf2} + B_{shf2}\dot{\theta}_{shf2} \quad (25)$$

$$T_{shf1}(s) = J_{shf1}s^2\theta_{shf1}(s) + B_{shf1}s\theta_{shf1}(s) \quad (26)$$

$$T_{shf2}(s) = J_{shf2}(s^2)\theta_{shf2}(s) + B_{shf2}s\theta_{shf2}(s) \quad (27)$$

By substituting (22) and (25) into (21), $T_{m1}(s)$ can be obtained as follow;

$$T_{m1}(s) = \left(\frac{1}{r_g}\left(J_{shf} + m_1d_1^1 + I_1 + m_2l_1^2\right)\theta_{shf1}(s)\right)s^2 + \left(\frac{1}{r_g}B_{shf}\theta_{shf1}(s)\right)s + \frac{1}{r_g}(m_1gd_1 + m_2gl_1)\theta_{shf1}(s) \quad (28)$$

Similarly $T_{m2}(s)$ can be obtained by substituting (23) and (27) into (21) as follows;

$$T_{m2} = (\frac{1}{r_g}(J_{shf} + m_2d_2^2 + I_2)s^2 + (\frac{1}{r_g}B_{shf}\theta_{shf2}(s))s + \frac{1}{r_g}(m_2gd_2\theta_{shf2}(s)) \quad (29)$$

The transfer function of the hip joint under Range of Motion (ROM) condition when one joint is moving and the other joint is fixed can be obtained by a substitute (28) into (16) and the results obtained as follow;

$$U_1(s) = \frac{\theta_{shf1}}{K_m r_g}\begin{bmatrix}(Ll_1^2m_2 + Ld_1^2m_1 + LI_1 + LJ_{shf})s^3 \\ +(Rl_1^2m_2 + Rd_1^2m_1 + RJ_{shf} \\ +RI_1 + LB_{shf1})s^2 \\ +(_1Lgm_2 + Ld_1gm_1 + RB_{shf} + K_br_g^2K_m)s \\ +Rl_1gm_2 \\ +Rd_1gm_1\end{bmatrix} \quad (30)$$

$$U_1(s) = \frac{\theta_{shf1}(z_{11}s^3+z_{12}s^2+z_{13}s+z_{14})}{y} \quad (31)$$

Where,

$$y = K_m r_g \quad (32)$$

$$z_{11} = Ll_1^2m_2 + Ld_1^2m_1 + LI_1 + LJ_{shf} \quad (33)$$

$$z_{12} = Rl_1^2m_2 + Rd_1^2m_1 + RJ_{shf} + RI_1 + LB_{shf} \quad (34)$$

$$z_{13} = l_1Lgm_2 + Ld_1gm_1 + RB_{shf} + K_br_g^2K_m \quad (35)$$

$$z_{14} = Rl_1gm_2 + Rd_1gm_1 \quad (36)$$

Similar for knee, the transfer function can be obtained by substituting (29) into (16) and the equation is shown as follow;

$$U_1(s) = \frac{\theta_{shf2}}{K_m r_g}\begin{bmatrix}(Ll_2^2m_2 + LJ_{shf} + LI_2)s^3 \\ +(Rd_2^2m_2 + RJ_{shf} \\ +RI_2 \\ +LB_{shf})s^2 + \\ (Ld_2gm_1 + RB_{shf} + \\ K_br_g^2K_m)s + Rd_2gm_2\end{bmatrix} \quad (37)$$

$$U_2(s) = \frac{\theta_{shf2}(z_{21}s^3+z_{22}s^2+z_{23}s+z_{24})}{y} \quad (38)$$

$$y = K_m r_g \quad (39)$$

$$z_{21} = Ll_2^2m_2 + Ld_2^2m_2 + LJ_{shf} + LI_2 \quad (40)$$

$$z_{22} = Rd_2^2m_2 + RJ_{shf} + RI_2 + LB_{shf} \quad (41)$$

$$z_{23} = Ld_2gm_1 + RB_{shf} + K_br_g^2K_{m_m} \quad (42)$$

$$z_{24} = Rd_2gm_2 \quad (43)$$

Finally, the transfer function of hip and knee joints can be expressed, as in (44) and (45) respectively.

$$G_1(s) = \frac{\theta_{shf1}(s)}{U_1(s)} = \frac{y}{z_{11}s^3+z_{12}s^2+z_{13}s+z_{14}} \quad (44)$$

$$G_2(s) = \frac{\theta_{shf2}(s)}{U_1(s)} = \frac{y}{z_{21}s^3+z_{22}s^2+z_{23}s+z_{24}} \quad (45)$$

IV. Controller Scheme

The decentralized control scheme was employed in the system. Hips and knee joints were controllled by individual PID controller as shown in Fig. 5.

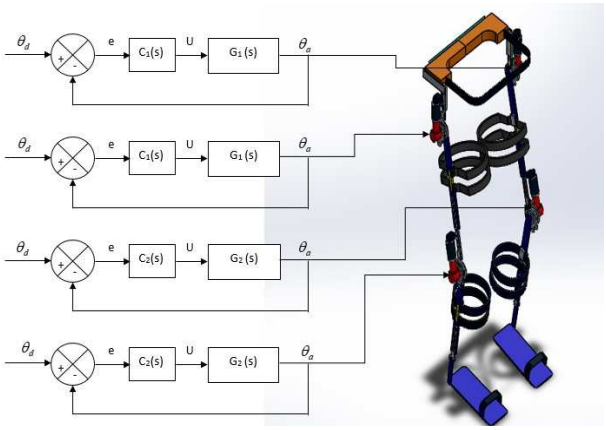

Fig. 5. PID Closed Loop Block Diagram

The control system is used to regulate the movement or position of mechanical hips and knee joints. Each of these joints has its own PID controller, which uses feedback mechanisms to ensure that the joints move or maintain positions as desired value. PID controllers were developed and employed on 3D model of WLLR in order to validate the derived dynamic model. This controller has three main parameters which are proportional, integral and derivative terms denoted by Kp, Ki and Kd respectively. Laplace transfer function of the PID controller is given as follows;

$$C(s) = \frac{U}{e} = K_p + \frac{1}{s}K_i + K_d s \quad (46)$$

$$C(s) = \frac{K_p s+K_i+K_d s^2}{s} \quad (47)$$

Where θ_d and θ_a are desired and actual trajectory, e represents the error of the control system, which is the difference between the desired and actual trajectory as expressed in the following;

$$e = \theta_d - \theta_a \quad (48)$$

The PID controller components for WLRR are tabulated as in Table I.

TABLE I. PID Block Components

Component	Transfer Function
PID Controller (Hip)	$C_1(s) = K_p + \frac{K_i}{s} + K_d s$
PID Controller (Knee)	$C_2(s) = K_p + \frac{K_i}{s} + K_d s$
Hip	$G_1(s) = \frac{y}{z_{11}s^3 + z_{12}s^2 + z_{13}s + z_{14}}$
Knee	$G_2(s) = \frac{y}{z_{21}s^3 + z_{22}s^2 + z_{23}s + z_{24}}$

The simulation parameters of the kinematic model are determined by geometry and material of the WLLR. These are obtained from 3D model mass properties, while the parameters of the motor model are obtained from the actual motor specification. Both WLLR and motor parameters are presented in Table II.

TABLE II. WLLR Link and DC Motor Parameters

Parameters			
WLLR		DC Motor	
m1(Kg)	0.95	L(H)	0.0024
m2(Kg)	0.31	R(ohm)	0.115
d1(m)	0.26	K_m(Nm/A)	0.0164
d2(m)	0.27	K_g	113
I1 (Kg.m^2)	0.009	K_b(V/rad^{-1})	0.001
I2(Kg.m^2)	0.004	J_{shf}(Kg.m^2)	0.0000139
g (ms^{-2})	9.81	B_{shf}	0.001

Conventional tuning method via the Ziegler-Nichols(ZN) second method was used to find the PID gain (Kp, Ki and Kd). The critical gain K_{cr} and critical period P_{cr} are important parameters that need to be determined first. Firstly, the value of the integral Ki and derivative Kd term is set to zero. A generic cubic polynomial method based Routh-Hurwitz stability criteria was used to find the K_{cr} value. The K_p value is set equal to K_{cr} when the system response showed sustained oscillation. Finally, the P_{cr} value can be obtained by dividing 2π with calculated angular velocity in the sustained frequency response.

TABLE III. PID Parameters

Parameters	Hip	Knee
Kp	3.25	0.95
Ki	24.95	9.58
Kd	0.11	0.02

The PID parameters obtained is shown as in Table III, and the step response for the hip and knee joint are illustrated as in Fig. 6 (a) and Fig. 6 (b).

TABLE IV. Performance of PID Controller

Results	Hip	Knee
Overshoot (%)	35.97	24.22
Settling Time (s)	8.02	3.25
Rise Time (s)	0.67	0.64
Steady-State Error	0.0011	0.0045

The model has been successfully tested by using PID (Ziegler–Nichols). Table IV shows the performance of both controllers for hip and knee. The rise time for PID (Ziegler–Nichols) controller is quite low for both hip and knee which demonstated the the system response are fast. Thus, the system can reach its desired setpoint or follow a reference signal more rapidly. Faster rise times are often desired in this applications where quick responses are essential. PID (Ziegler–Nichols) controller also has a lower Steady-State

error value for both hip and knee which indicates the system has reached a stable condition.Minimal steady-state error is crucial in achieving precise control. Despite these advantages, PID (Ziegler–Nichols) has high overshoot. which makes the output temporarily exceed the desired value before settling. In this work, PID controller is primarily employed to validate whether the system modeling and its derivatives can accurately represent the system's behavior and its controllability. Therefore, it is possible to work on reducing or improving overshoot later.

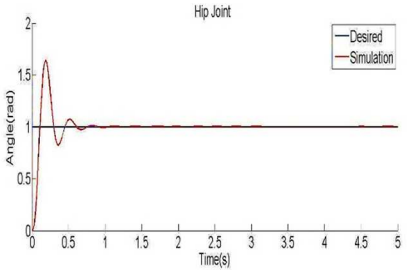

(a)

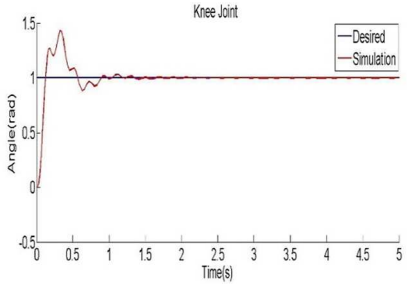

(b)

Fig. 6. Step Response (a)Hip (b) Knee

V. Experimental Results Via SimMechanics

The behaviour of the WLLR was investigated in virtual environments to verify the dynamic model of WLRR. The dynamic model was simulated by using MATLAB SimMechanic platform as shown in Fig. 7. All the parameters in Table II and Table III are added to the position control algorithm in Fig. 5.

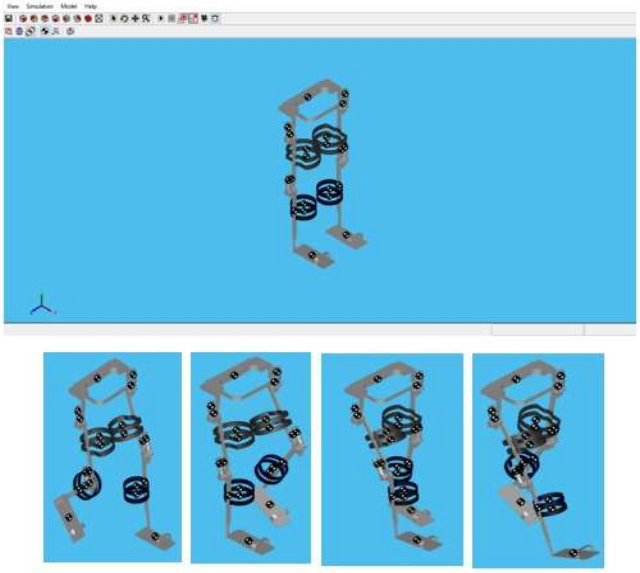

Fig. 7. SimMechanic Model (Simulation Platform)

The dynamic model was tested experimentally via the performance of the PID controller, namely ROM. In the ROM condition, the performance of each joint was observed, while the other joints were fixed [23]. The sine wave motion was applied to the hip and knee for both legs to perform ROM condition. The ROM angle applied to the hip was between -45.84° and 45.84° (-0.8 rad and 0.8 rad) while for the knee the range was between -85.37°and -85.37°(-1.49 radand 1.49 rad).

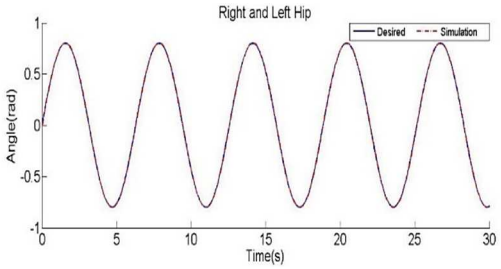

(a)

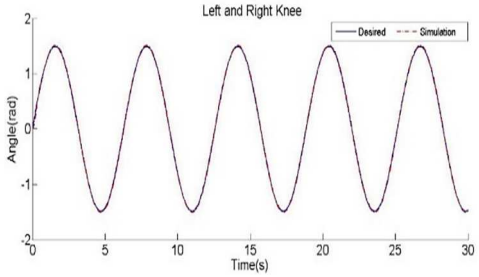

(b)

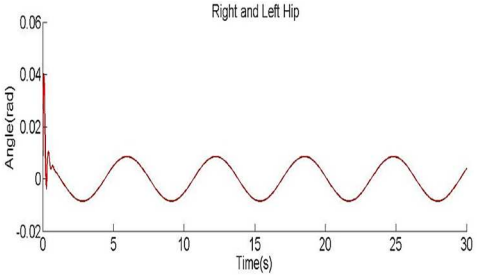

(c)

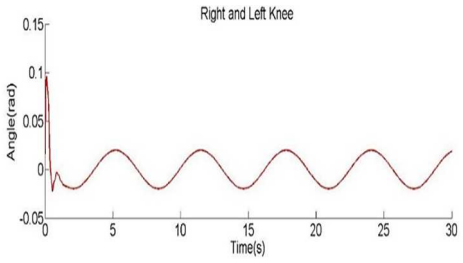

(d)

Fig. 8. Tracking Error in ROM condition (a) Right and Left Hip (b) Right and Left Knee (c) Right and Left Hip Tracking Error (d) Right and Left Knee Tracking Error

Fig. 8 compared the trajectory performance of hip and knee joint to perform ROM condition. In the ROM condition,

both legs of hip and knee showed the same tracking performance respectively. The reason is because both legs has the same kinematic structure and used the same PID parameters.

The results showed that the tuned PID parameters and the derived dynamic model for the hip and knee of both legs are able to make the WLLR follow the desired ROM trajectory. As depicted in Fig. 8(c) and 8(d), the position tracking error for the ROM condition of the right and left hip and knee exhibited minimal errors that are negligible.

VI. Conclusion

In this study, the dynamic model of the proposed design is modelled mathematically by utilizing Lagrangian formulation. The dynamic model was verified by implementing the PID controller on the WLRR. The behaviour of the WLLR was observed through SimMechanics simulations. The results showed that WLRR followed the desired ROM trajectory sine wave motion that was set as desired output with acceptable errors. The simulated model and PID controller are well reflected in the dynamic model where the rise time and steady state error are minimum for both hip and knee which indicates that the WLLR has fast response and a good tracking performance.

Conflict of Interests

The author(s) declared no potential conflicts of interest with respect to the research, authorship, and/or publication of this article.

Acknowledgments

The authors wish to thank the Sarawak Research and Development Council (SRDC) and Universiti Malaysia Sarawak (UNIMAS) for providing the research grant and facilities. This research is supported using SRDC Grant, Id No: RDCRG/CAT/2019/22.

References

[1] Iandolo, R., Marini, F., Semprini, M., Laffranchi, M., Mugnosso, M., Cherif, A., De Michieli, L., Chiappalone, M., & Zenzeri, J. (2019). Perspectives and challenges in robotic neurorehabilitation. *Applied Sciences (Switzerland)*, *9*(15). https://doi.org/10.3390/app9153183

[2] Zhang, Xue, Yue, Z., & Wang, J. (2017). Robotics in Lower-Limb Rehabilitation after Stroke. *Behavioural Neurology*, *2017*. https://doi.org/10.1155/2017/3731802

[3] Hidayah, R., Bishop, L., Jin, X., Chamarthy, S., Stein, J., & Agrawal, S. K. (2020). Gait Adaptation Using a Cable-Driven Active Leg Exoskeleton (C-ALEX) with PostStroke Participants. IEEE Transactions on Neural Systems and Rehabilitation Engineering, 28(9), 1984–1993.

[4] Bartenbach, V., Wyss, D., Seuret, D. et al. (2015). A lower limb exoskeleton research platform to investigate human-robot interaction. *IEEE International Conference on Rehabilitation Robotics*, 600–605.

[5] Liu, Q., Zuo, J., Zhu, C., & Xie, S. Q. (2020). Design and control of soft rehabilitation robots actuated by pneumatic muscles: State of the art. Future Generation

[6] Computer Systems,Ghaddar, R., & Mohammad, A. (2019). A Review of Lower Limb Exoskeleton Assistive Devices for Sit-to-Stand and Gait Motion. *International Journal of Current Engineering and Technology*, *9*(1), 105–111.

[7] Chang, T. H., Koizumi, S., Nabae, H., Endo, G., Suzumori, K., Hatakeyama, K., Chida, S., & Shimada, Y. (2020). A Wearable Ankle Exercise Device for Deep Vein Thrombosis Prevention Using Thin McKibben Muscles. Proceedings of the IEEE RAS and EMBS International Conference on Biomedical Robotics and Biomechatronics, 42–47.

[8] Bortole, M., Venkatakrishnan, A., Zhu et al. (2015). The H2 robotic exoskeleton for gait rehabilitation after stroke: Early findings from a clinical study Wearable robotics in clinical testing. *Journal of NeuroEngineering and Rehabilitation*, *12*(1): 1–14.

[9] Chen, B., Zhong, C., Zhao, X et al. (2017). A wearable exoskeleton suit for motion assistance to paralyzed patients. *Journal of Orthopaedic Translation*, *11*(3): 7–18.

[10] Bartenbach, V., Wyss, D., Seuret, D. et al. (2015). A lower limb exoskeleton research platform to investigate human-robot interaction. *IEEE International Conference on Rehabilitation Robotics*, 600–605.

[11] Gan, D., Qiu, S., Guan, Z. et al. (2016). Development of a exoskeleton robot for lower limb rehabilitation. *International Conference on Advanced Robotics and Mechatronics*, 312–317.

[12] Kim, S & Bae, J. (2014). Development of a lower extremity exoskeleton system for human-robot interaction. *International Conference on Ubiquitous Robots and Ambient Intelligence*, 132–135.

[13] Kolakowsky-Hayner, S. A. (2013). Safety and Feasibility of using the EksoTM Bionic Exoskeleton to Aid Ambulation after Spinal Cord Injury. *Journal of Spine*.

[14] Chen, C., Zheng, D., Peng, A. et.al.. (2013). Flexible design of a wearable lower limb exoskeleton robot. *IEEE International Conference on Robotics and Biomimetics*, 209–214.

[15] Sankai, Y. (2010). HAL: Hybrid assistive limb based on cybernics. *Springer Tracts in Advanced Robotics*, *66:*25–34.

[16] Z. Zhang, "An Adaptive Lower Limb Rehabilitation Exoskeleton Robot Designing Scheme," 2022 3rd International Conference on Intelligent Design (ICID), Xi'an, China, 2022, pp. 244-248, doi: 10.1109/ICID57362.2022.9969720.

[17] Guo, Q., Li, S., & Jiang, D. (2015). A Lower Extremity Exoskeleton: Human-Machine Coupled Modeling, Robust Control Design, Simulation, and Overload-Carrying Experiment. *Mathematical Problems in Engineering*, *2015*.

[18] Ferrati, F., Bortoletto, R., & Pagello, E. (2013). Virtual modelling of a real exoskeleton constrained to a human musculoskeletal model. *Lecture Notes in Computer Science (Including Subseries Lecture Notes in Artificial Intelligence and Lecture Notes in Bioinformatics)*, *8064 LNAI*, 96–107.

[19] Y. Liu, J. Zhang and W. -H. Liao, "Dynamic Modeling and Identification of Wearable Lower Limb Rehabilitation Exoskeleton Robots," 2022 4th International Conference on Control and Robotics (ICCR), Guangzhou, China, 2022, pp. 217-221, doi: 10.1109/ICCR55715.2022.10053854.

[20] Y. Li et al., "Dynamic Parameter Identification of a Human-Exoskeleton System With the Motor Torque Data," in IEEE Transactions on Medical Robotics and Bionics, vol. 4, no. 1, pp. 206-218, Feb. 2022, doi: 10.1109/TMRB.2021.3137970.

[21] Bartenbach, V., Gort, M., & Riener, R. (2016). Concept and design of a modular lower limb exoskeleton. *Proceedings of the IEEE RAS and EMBS International Conference on Biomedical Robotics and Biomechatronics*, 649–654.

[22] Kainz, H., Carty, C. P., Lloyd, D et al. (2017). Effects of hip joint centre mislocation on gait kinematics of children with cerebral palsy calculated using patient-specific direct and inverse kinematic models. Gait and Posture, 57:154–160.

[23] Amiri, M. S., Ramli, R., & Ibrahim, M. F. (2019). Hybrid design of PID controller for four DoF lower limb exoskeleton. Applied Mathematical Modelling, 72: 17–27.

[24] Chachati, L & Hasan, A. (2018). Designing and implementing an electronic system to control moving orthosis virtual mechanical system to emulate lower limb. *Cogent Engineering*, *5*(1).